

HIGH STRENGTH TO WEIGHT ALUMINUM -  
18 WEIGHT PERCENT MAGNESIUM ALLOY  
THROUGH THERMAL MECHANICAL PROCESSING

Frank George Ness

SHRI LALJI LIBRARY  
JALALI POSTGRADUATE SCHOOL

# NAVAL POSTGRADUATE SCHOOL

## Monterey, California



# THESIS

HIGH STRENGTH TO WEIGHT ALUMINUM -  
18 WEIGHT PERCENT MAGNESIUM ALLOY  
THROUGH THERMAL MECHANICAL PROCESSING

by

Frank George Ness, Jr.

December 1976

Thesis Advisor:

Terry R. McNelley

Approved for public release; distribution unlimited.

T177101



## UNCLASSIFIED

SECURITY CLASSIFICATION OF THIS PAGE (When Data Entered)

REPORT DOCUMENTATION PAGE		READ INSTRUCTIONS BEFORE COMPLETING FORM
1. REPORT NUMBER	2. GOVT ACCESSION NO.	3. RECIPIENT'S CATALOG NUMBER
4. TITLE (and Subtitle)  High Strength to Weight Aluminum - 18 Weight Percent Magnesium Alloy Through Thermal Mechanical Processing		5. TYPE OF REPORT & PERIOD COVERED  Master's Thesis December 1976
7. AUTHOR(s)  Frank George Ness, Jr.		6. PERFORMING ORG. REPORT NUMBER
9. PERFORMING ORGANIZATION NAME AND ADDRESS  Naval Postgraduate School Monterey, Ca. 93940		10. PROGRAM ELEMENT, PROJECT, TASK AREA & WORK UNIT NUMBERS
11. CONTROLLING OFFICE NAME AND ADDRESS  Naval Postgraduate School Monterey, Ca 93940		12. REPORT DATE  December, 1976
14. MONITORING AGENCY NAME & ADDRESS (if different from Controlling Office)  Naval Postgraduate School Monterey, Ca 93940		13. NUMBER OF PAGES  62
16. DISTRIBUTION STATEMENT (of this Report)  Approved to public release; distribution unlimited		15a. DECLASSIFICATION/DOWNGRADING SCHEDULE
17. DISTRIBUTION STATEMENT (of the abstract entered in Block 20, if different from Report)		
18. SUPPLEMENTARY NOTES		
19. KEY WORDS (Continue on reverse side if necessary and identify by block number)  Thermal Mechanical Processing		
20. ABSTRACT (Continue on reverse side if necessary and identify by block number)  An Aluminum-18 weight percent Magnesium alloy was prepared by casting and then warm rolling at 425°C to 94% true strain. This alloy was compression tested at six strain rates from 0.00664 per minute to 0.332 per minute and at eight temperatures ranging from 25°C to 425°C. The most significant result is that a warm rolled Aluminum-18 weight percent Magnesium alloy can exhibit compressive strengths in excess of 95 ksi, in a material of 10% lower density than commercial high strength Aluminum alloys.		



UNCLASSIFIED

SECURITY CLASSIFICATION OF THIS PAGE/When Data Entered.

Furthermore, one can envision a thermal mechanical process involving warm working followed by cold working at room temperature whereby one can attain an ultimate tensile strength greater than 90 ksi. Additionally, superplastic behavior at elevated temperatures was manifest in the relatively high value of strain rate sensitivity and by the value of the activation energy for deformation.



HIGH STRENGTH TO WEIGHT ALUMINUM-18 WEIGHT PERCENT  
MAGNESIUM ALLOY THROUGH THERMAL MECHANICAL PROCESSING

by

*Frank G. Ness Jr.*  
Lieutenant, United States Navy  
Bachelor of Science in Mechanical Engineering,  
University of Utah, 1968

Submitted in partial fulfillment of the  
requirements for the degree of

MASTER OF SCIENCE IN APPLIED SCIENCE

from the  
NAVAL POSTGRADUATE SCHOOL  
December 1976



## ABSTRACT

An Aluminum-18 weight percent Magnesium alloy was prepared by casting and then warm rolling at  $425^{\circ}\text{C}$  to 94% true strain. This alloy was compression tested at six strain rates from 0.00664 per minute to 0.332 per minute and at eight temperatures ranging from  $25^{\circ}\text{C}$  to  $425^{\circ}\text{C}$ . The most significant result is that a warm rolled Aluminum-18 weight percent Magnesium alloy can exhibit compressive strengths in excess of 95 ksi, in a material of 10% lower density than commercial high strength Aluminum alloys. Furthermore, one can envision a thermal mechanical process involving warm working followed by cold working at room temperature whereby one can attain an ultimate tensile strength greater than 90 ksi. Additionally, superplastic behavior at elevated temperatures was manifest in the relatively high value of strain rate sensitivity and by the value of the activation energy for deformation.

100 CHILD  
1000 CIGARETTE

## TABLE OF CONTENTS

LIST OF FIGURES.....	7
I. INTRODUCTION.....	8
II. EXPERIMENTAL METHODS.....	10
A. ALLOY SELECTION.....	10
B. SPECIMEN PREPARATION.....	10
C. EQUIPMENT DESCRIPTION.....	14
D. TEST PROCEDURE.....	15
E. MICROSCOPIC ANALYSIS.....	16
III. RESULTS AND DISCUSSION.....	18
A. MICROSTRUCTURAL ANALYSIS.....	18
B. AMBIENT TEMPERATURE CHARACTERISTICS.....	19
C. ELEVATED TEMPERATURE CHARACTERISTICS.....	20
D. FOLLOW ON ANALYSIS.....	26
IV. CONCLUSIONS AND RECOMMENDATIONS.....	27
A. CONCLUDING COMMENTS.....	27
B. RECOMMENDATIONS.....	28
Appendix A: ALUMINUM-MAGNESIUM CASTING PROCEDURES.....	59
LIST OF REFERENCES.....	60
INITIAL DISTRIBUTION LIST.....	62



## LIST OF FIGURES

1.	Aluminum-Magnesium phase diagram.....	29
2.	Melting furnace and clay graphite crucible.....	30
3.	Split bronze mold, 1 inch square by 12 inches.....	31
4.	Warming furnace and rolling mill.....	32
5.	Instron Model TT-D floor model testing machine.....	33
6.	Special compression test assembly with support ring and retaining clips.....	34
7.	Marshall split furnace.....	35
8.	S4-10 Stereoscan Scanning Electron Microscope with PGT-1000 Micro Analysis System.....	36
9.	SEM photograph of as cast material, 610X.....	37
10.	SEM photograph #1 of as cast material, 1,200X.....	38
11.	SEM photograph #2 of as cast material, 1,200X.....	39
12.	SEM photograph #3 of as cast material, 1,200X.....	40
13.	SEM photograph #1 of as cast material, 2,400X.....	41
14.	SEM photograph #2 of as cast material, 2,400X.....	42
15.	SEM photograph of warm rolled material, 1,280X.....	43
16.	SEM photograph of warm rolled material, 2,550X.....	44
17.	SEM photograph of warm rolled material, 6,300X.....	45
18.	SEM photograph of warm rolled material, 13,000X.....	46
19.	True stress vs. true strain for as cast (*)	



and warm rolled (+) material.....	47
20. True stress vs. true strain for warm rolled material at two cross head speeds and temperatures to 245° C.....	48
21. True stress vs. true strain for warm rolled material at two cross head speeds and temperatures to 420° C.....	49
22. Flow stress vs. temperature at a true strain of 0.15 for six strain rates.....	50
23. Work hardening exponent (n) and strain rate sensitivity (m) vs. fraction of abs. melting temp.....	51
24. Elastic Modulus (E) vs temperature, (11) .....	52
25. Natural log of strain rate vs. reciprocal absolute temperature for various values of ( $\sigma/E$ ) ...	53
26. Temperature vs. percentage beta phase intermetallic.....	54
27. SEM photograph of a warm rolled specimen following compression testing, 1,225X.....	55
28. SEM photograph of a warm rolled specimen following compression testing, 2,500X.....	56
29. SEM photograph of a warm rolled specimen following compression testing, 6,300X.....	57
30. SEM photograph of a warm rolled specimen following compression testing, 12,500X.....	58



## I. INTRODUCTION

The objective of this research project was to investigate the metallurgical and mechanical properties of a warm rolled proeutectic Aluminum-Magnesium alloy, from room temperature to just below the melting point. This was done with the hope that sufficient preliminary work could be accomplished to promote future research at the Naval Postgraduate School in the field of thermal mechanical processing of Aluminum-Magnesium alloys. Because of the current need for high strength to weight materials in naval applications, the Aluminum-Magnesium system was chosen. The intent here was to reduce density and thus promote an improvement in the strength to weight ratio over other high strength Aluminum alloys. Because so little research has been done on Aluminum alloys containing greater than 10 weight percent Magnesium, and because an 18 weight percent Magnesium alloy will afford nearly equal volume fractions of the two phases present, as seen in figure 1, an 18 weight percent Magnesium alloy was selected.

The warm rolling concept used in this project is the same as that employed by Bly, Sherby, and Young (1) wherein improved ductility and strength were manifest in a eutectoid carbon steel through warm rolling. The warm rolling procedure used in this project is that thermal mechanical process in which a two phase system is heated to about 96% of the absolute melting temperature and then deformed in a rolling mill until a true strain of approximately 100%, or greater, is achieved. Bly, Sherby, and Young stated (1) that the ideal structure would be one of finely spheroidized particles, uniformly distributed throughout the matrix of



this carbon steel. It was found that ductility could be increased from 1% to 10% and that the yield stress was increased through strain hardening by about 35%. It was these results which prompted the warm rolling techniques with the selected Aluminum-Magnesium system.

Based upon the results of Bly, Sherby, and Young (1), one would expect a warm rolled Aluminum-18 weight percent Magnesium alloy to exhibit a fine, two phase structure comprised of colonies of small (about 0.5 micron) beta phase intermetallic particles dispersed in the Aluminum rich alpha solid solution which is readily work hardenable at room temperature. This results from the constraints imposed by the fine particles, in this metastable solid solution, on dislocation motion. Further, one might expect to see the onset of superplasticity, as defined by Sherby (2), at elevated temperatures. This is the result of the high degree of strain rate sensitivity, observed at higher temperatures, which was induced by the intrinsically fine grain structure.

Though this research project has but scratched the surface in a relatively new field of metallurgy, with profound potential, the original goal has more than just been achieved. Now that the groundwork has been laid and a basis has been established, it is recommended that research in this area be continued, if not accelerated, to understand further the microstructural phenomenology, and to optimize the thermal mechanical processing of high strength to weight Aluminum-Magnesium alloys for the Navy of tomorrow.



## II. EXPERIMENTAL METHODS

### A. ALLOY SELECTION

An Aluminum alloy containing approximately 18 weight percent Magnesium was chosen for the purpose of this investigation. The rationale behind this decision was that alloys containing higher weight percentages of Magnesium were too brittle. This brittleness precluded the attainment of the desired 100 percent true strain during the warm rolling process. Lower weight percentages of Magnesium, on the other hand, afforded a lesser weight percentage of the beta phase intermetallic ( $Al_3Mg_2$ ), and therefore strength would be expected to be less than that found in alloys with a greater Magnesium content. This relationship between the Aluminum rich alpha phase solid solution and the beta phase intermetallic can be seen in figure 1.

### B. SPECIMEN PREPARATION

All of the experimental methods described in this chapter were conducted on specimens produced and prepared in the Naval Postgraduate School Material Science Laboratory. It should be stated at the outset that due to the propensity for Magnesium to burn at elevated temperatures, and the hazards of this type of fire (3), considerable time was expended in procedure development before useable samples were produced.



Preliminary attempts at melting were done using small amounts (a few ounces) of Aluminum strips and Magnesium turnings. These attempts invariably resulted in Magnesium fires, and all that remained in the crucible was a mass of Aluminum Oxide, Magnesium Oxide, and some Aluminum metal. These fires were the result of high temperature, the presence of Oxygen, and the large degree of surface area on the Magnesium turnings.

In order to alleviate the latter two problems, a dry Argon purge was used to reduce the amount of Oxygen present in the furnace; also, pure Magnesium in the form of clean, right circular cylinders, 1 to 2 inches in length and 0.5 to 1 inch in diameter were used. With these changes, castings could be made but were of poor quality due to casting flaws and excessive dross. It was found that if the furnace temperature was kept too low, very little mixing could be accomplished without the melt beginning to solidify. If the temperature was too high, there was a noticeable increase in the porosity in the castings. Thus an optimal furnace temperature of 750° C was used for casting purposes.

The excessive dross, mentioned above, is caused by the oxidation of the hot melt. By applying a proprietary flux ("Coverall #33FF", purchased from the Industrial Foundry Supply Co., Oakland, Calif.) produced especially for Aluminum-Magnesium alloys, the formation of the dross was nearly eliminated.

Finally, by the eighth casting, an acceptable sample relatively free of impurities and casting flaws was produced. To achieve this end, the step by step procedure provided in Appendix A was used and basically involves the following: The Carbon crucible (approximately 9 cubic inches in volume) was preheated at 250° C for one hour to ensure that adequate outgassing had occurred. The crucible was



then removed from the warming furnace, charged with Aluminum (greater than .999 pure) in the form of 0.5 to 1 inch cubes. The crucible was then placed into the preheated electric furnace shown in figure 2. A dry Argon purge of approximately two standard cubic feet per hour was bled into the furnace at the commencement of preheat and continued throughout the melting procedure. As mentioned earlier, this was done in order to reduce the Oxygen content within the melting furnace.

In about one hour the crucible with the molten Aluminum was removed from the furnace and fluxed with about 0.2 ounce of "Coverall #33FF". Pure Magnesium in the form mentioned above was then submerged in the molten Aluminum, using stainless steel tongs until it too had melted. The crucible was then returned to the furnace.

After about half an hour, the crucible was withdrawn, and the melt was again fluxed with approximately 0.2 ounce of "Coverall #33FF" and carefully stirred. The accumulated dross was then removed from the surface of the melt using the stainless steel stirring rod, and the crucible was returned to the furnace and allowed to stabilize with the furnace temperature. At this point the melt was removed and was rapidly cast into the 1 inch square by 12 inch bronze mold, shown in figure 3. This mold was fabricated in the Mechanical Engineering machine shop and was constructed with a longitudinal split to facilitate removal of the casting when cooled.



When pouring was complete, the mold was rapidly quenched to ambient temperature by immersing it in a large container of water. This was done to promote the finest possible microstructure prior to the warm rolling process. The casting was then sent to the machine shop for cutting into quarters about the longitudinal axis, and trimming into samples of uniform cross section, about 0.40 inch on a side and roughly 3 inches in length.

Following density measurements, one sample was retained for testing in the as cast condition, and the remainder were placed in a warming furnace heated to  $425^{\circ}\text{C}$ . This is  $26^{\circ}\text{C}$  below the eutectic temperature.

The specimens were equilibrated at this temperature and the billets were then passed through the rolling mill shown in figure 4. These passes were made at a rate of 2 inches per minute and a reduction of 0.005 inch per pass. The billets were rotated a quarter of a turn after each pass in an attempt to achieve uniform working and to maintain a square cross section. The billet was returned to the warming furnace, shown in figure 4, after passes at one thickness setting and allowed to stabilize. The rolling mill was adjusted to the next lower thickness setting, and another four passes were made.

Although the intent was to achieve a minimum of 100% true strain by warm rolling, the procedure was terminated at approximately 94% true strain. This was done because fine cracks began to appear on the surface of the rolled billets. It is believed that this cracking is the result of the hot billets coming into abrupt contact with the ambient temperature rollers, thus giving rise to severe thermal gradients at the surface. This effect could be reduced or possibly eliminated if the rollers were maintained at the



warm rolling temperature, or better yet if the billets were formed in a hot extrusion process where the extrusion tooling was maintained at the proper temperature.

Following the warm rolling procedure, the billets were cut and trimmed into parallelepiped shaped test specimens roughly 0.35 inch in length and 0.25 inch on a side. At this point the specimens were ready for testing.

### C. EQUIPMENT DESCRIPTION

All mechanical testing was conducted on the Instron Model TT-D floor model testing machine shown in figure 5. This machine is capable of applying and recording loads up to 20000 pounds with crosshead speeds from 0.002 inch per minute to 20 inches per minute.

The compression test assembly, adapted from an original design by Drs. C. Young and D. Bly, Stanford University, was designed to be compatible with the Instron testing machine. The compression assembly shown in figure 6 consists of a one inch diameter Haynes 188 punch and a three inch outside diameter Inconel cylinder with a 1.010 inch bore. The punch fits inside the test cylinder and slides on two machined lands inside the cylinder. Both the punch and the cylinder head have machined recesses to accommodate the two Tungsten Carbide platens above and below the test specimens. Because the specimens were tested at elevated temperatures, a special support ring and three retaining springs were constructed to hold the upper platen in place.

To conduct the compression tests at various temperatures the Marshall split furnace in figure 7, capable of temperatures to 1200° C, was utilized. Control of the



furnace was provided by a Model #49 Omega proportioning control unit. Temperature variance was limited to  $\pm 5^\circ\text{C}$ . In addition, a Chromel-Alumel thermocouple provided a backup temperature monitoring capability through a Leeds Northrup model #8690 millivolt potentiometer.

#### D. TEST PROCEDURE

A total of 24 specimens were tested at eight temperatures, from  $25^\circ\text{C}$  to  $425^\circ\text{C}$ , and at six crosshead speeds from 0.002 inch per minute to 0.100 inch per minute. It should be noted that each specimen was used for two different strain rates. The test apparatus was brought to the desired temperature and allowed to stabilize before placing the specimen in the compression chamber.

In order to reduce the effects of transverse stress (ie., triaxiality) induced by the friction between the specimen and the platens during compression, commercial grade Teflon tape was applied to the contact surfaces of the specimen for tests at temperatures up to  $100^\circ\text{C}$ . Above this temperature a commercial high temperature lubricant containing Molybdenum Disulfide was applied.

A machine curve was generated in order to determine the intrinsic load-deflection characteristics of the Instron test machine. The results of this test indicated a spring constant of 250,726 pounds per inch.



## E. MICROSCOPIC ANALYSIS

In order to analyze the microstructural and topological characteristics of the three types of samples, ie., as cast, warm rolled, and post compression test, specimens were prepared for microscopic analysis. Samples to be analyzed were trimmed to about 0.25 inch on a side and then abraded on successively finer sheets of emery paper to 3/0. The specimens were then polished by hand using slurries of Alumina and water on a stationary polishing cloth. The final grit size was 0.05 micron.

The specimens were etched with a 5% hydrofluoric acid solution in accordance with the procedures set forth in reference 4. The specimens which were to be analyzed in the Scanning Electron Microscope (SEM) were attached to SEM mounting stubs with conductive paint. The specimens were then placed in the S4-10 Stereoscan Scanning Electron Microscope seen in figure 8 (Cambridge Scientific Instruments Limited). Using magnifications of 610X to 13,000X, the surface of the three specimen types were viewed and photographed.



The photomicrographs were examined with the quantitative microscopy techniques "Grain Boundary Intercept" and "Lineal Fraction", as described in reference 5, to determine the average grain sizes and volume fractions of the two phases present.

Because the Scanning Electron Microscope is capable of providing an energy dispersive X-ray analysis through the PGT-1000 Micro Analysis System (Princeton Gamma-Tech) shown in figure 8, a check for impurity elements was also made using the Pulse Height Analyzer mode of operation.



### III. RESULTS AND DISCUSSION

#### A. MICROSTRUCTURAL ANALYSIS

The microstructure of the as cast alloy is shown in figure 9, which is a photomicrograph taken at a magnification of 610X on the Scanning Electron Microscope (SEM). One can observe that the beta phase intermetallic has been preferentially attacked, and there appears to be a homogeneous distribution of these large particles throughout the Aluminum rich alpha phase solid solution. Figures 10, 11, and 12, taken at 1,200X, provide a further look at the size, shape, and distribution of the intermetallic phase in the solid solution matrix. By applying the quantitative techniques mentioned earlier, these three figures revealed an average particle size of about ten microns and a volume percentage of about 23% beta phase. The 23 volume percentage beta corresponds to the equilibrium amount predicted from the phase diagram (figure 1) using the warm rolling temperature of 425° C. Furthermore, the well rounded, irregularly shaped particles apparent in figures 13 and 14 correspond to the description of this intermetallic given in reference 6.



Figures 15 through 18 are SEM photomicrographs at magnifications up to 13,000X showing the results of the warm rolling process. In figures 15 and 16 one can see the very fine intermetallic particles distributed in clusters throughout the alpha phase solid solution. It also appears that some particles have formed preferentially along the alpha solid solution boundaries as observed in figure 16.

Figure 18 is a SEM photomicrograph taken at a magnification of 13,000X; and although the resolution at this magnification is poor, one can observe that the particles are extremely fine (about 0.45 micron average) and inhomogeneous in shape and relative size.

#### B. AMBIENT TEMPERATURE CHARACTERISTICS

The results obtained from the compression testing of the warm rolled material were most gratifying. To begin with, a comparison was made between the as cast and the warm rolled material. The results of this comparison are provided as figure 19. Though the yield stress for each material is about the same, the flow stress (for a true strain of 0.21) is about 30% greater with the warm rolled material. Furthermore, one can see that by warm rolling the as cast material and then cold working it to a true strain of about 0.30, one can achieve compressive strengths in excess of 95 ksi. The profound significance of these results is that one can envision a thermal mechanical process which would include an optimal degree of warm rolling and subsequent cold working wherein ultimate tensile strengths of 90 to 95 ksi can be achieved in a material which is less dense than commercial high strength Aluminum alloys. The combination of the high strength and less dense characteristics would



yield about a 20% increase in the strength to weight ratio over the conventional 7075-T6 type Aluminum alloys currently in use. In addition one would expect good toughness properties due to the strongly work hardenable characteristics of this material.

### C. ELEVATED TEMPERATURE CHARACTERISTICS

The effects observed in the compression testing of this material at various temperatures and strain rates are shown in figures 20 and 21. These plots clearly demonstrate a tendency towards strain softening at temperatures above 245° C. This characteristic will be discussed in greater detail later in this chapter. By utilizing the information from these figures, a plot of flow stress (at 0.15 true strain) versus temperature was generated in order to observe the temperature and strain rate dependence on flow stress. Figure 22 provides the results of this examination. It is quite apparent that for temperatures between 185° C and the melting point there exists a characteristic pattern between flow stress, temperature, and strain rate. Between 50° C and 150° C, on the other hand, it appears that there does exist some degree of strain aging occurring wherein the Magnesium atoms in the alpha phase solid solution are inhibiting dislocation motion. This is manifest in the slight increase in flow stress with a small increase in temperature in this region. This was also evidenced by the Portevin-LeChatlier effect (serrated flow curves) witnessed during compression testing in this particular temperature range.



The next step taken in the characterization of this material was to evaluate the degree of strain hardening and strain rate sensitivity exhibited by this alloy under varying temperature conditions. Dieter (7) describes the relationship between true stress and true strain as follows:

$$\sigma = K \epsilon^n \quad (1)$$

where  $\sigma$  is the true stress;  $\epsilon$  the true strain;  $K$ , the strength coefficient; and  $n$  is the strain hardening exponent. By applying a least squares fit of a power curve approximation to the stress-strain data obtained for various temperatures, figure 23 was produced. One can observe that for temperatures of  $100^{\circ}\text{C}$  and below this material is quite ductile and very work hardenable as the  $n$  values of 0.35 to 0.40 would indicate. Based upon the tensile instability concept from Dieter (7), one would expect a uniform elongation of  $\epsilon = 0.40$  before the onset of necking. It is because of this that one can envision a thermal mechanical process in which the material is first warm rolled and then cold worked to a true strain of 0.30. One would logically expect this material to have 0.10 more uniform deformation remaining with an ultimate tensile strength upwards of 95 ksi.

In an attempt to determine the extent of superplasticity exhibited by this material, the following equation, also from Dieter (7), was utilized:

$$\sigma = C \dot{\epsilon}^m \quad (2)$$

Here again  $\sigma$  is the true stress,  $\dot{\epsilon}$  is the strain rate,  $C$  is a constant, and  $m$  is the strain rate sensitivity exponent. Again, a least squares fit to a power curve approximation was used in determining values of  $m$  at various temperatures. A look at figure 23 shows that for



temperatures above about 300° C,  $m$  values between 0.30 and 0.40 were achieved. Since superplastic metals and alloys generally exhibit strain rate sensitivity exponent ( $m$ ) values in the range of 0.40 to 0.60, as stated in reference (2), it appears that superplastic behavior was achieved.

Equation (2) is only valid for a specified constant temperature, so in order to analyze the interrelationship between flow stress, strain rate, and temperature, the following equation from Sherby and Burke (8) was utilized:

$$\dot{\epsilon} = K' (\sigma/E)^{1/m} \exp(-Q/RT) \quad (3)$$

again  $\dot{\epsilon}$  is strain rate,  $\sigma/E$  is modulus compensated flow stress,  $Q$  is the activation energy for dislocation motion,  $T$  is the absolute temperature,  $R$  is the Universal Gas Constant,  $m$  is the strain rate sensitivity, and  $K'$  is a constant. The use of equation (3) seems to be proper in that Meyers, Shyne, and Sherby (9) have demonstrated that Aluminum and Aluminum alloys adhere to this formulation.

In order to investigate the cogency of this argument for this material, modulus compensated flow stresses were generated using the information from figure 24, which plots the dynamic elastic modulus for Aluminum versus temperature. Following this, a plot was constructed of the natural log of strain rate versus the reciprocal of absolute temperature for various values of modulus compensated flow stress. These results are shown in figure 25.



One would expect that for equation (3) to be valid, the plots in figure 25 should be linear, with slopes equal to  $-Q/R$ , but figure 25 does not bear this out. Because of the consistent pattern observed, which varies from that of a straight line, a nonlinear relationship is depicted. It is believed that this variance from a straight line function can be attributed to several factors. First, the fraction of the beta phase present is a function of temperature. This results because the concentration of Magnesium in the alpha phase solid solution also varies with temperature.



Barrett, Nix, and Tetelman (10) have shown that under equilibrium conditions the fraction of impurity atoms present in the alpha solid solution can be expressed by equation (4).

$$C_\alpha = \exp(-\Delta E/kT) \quad (4)$$

$C_\alpha$  is the concentration of Magnesium atoms in the solid solution,  $\Delta E$  is the change in energy associated with the addition of Magnesium atoms to the alpha solid solution,  $k$  is Boltzmann's constant, and  $T$  is the absolute temperature. Now by applying the lever rule to the tie line principle in conjunction with figure 1, the fraction of beta phase present can be expressed as follows:

$$f_\beta = \frac{C_0 - C_\alpha}{C_\beta - C_\alpha} = \frac{C_0 - \exp(-\Delta E/kT)}{C_\beta - \exp(-\Delta E/kT)} \quad (5)$$

Here,  $C_0$  is the over all Magnesium concentration,  $C_\beta$  is the concentration of Magnesium in the beta phase, and  $f_\beta$  is the fraction of beta phase. A graphic representation of this analysis is provided in figure 26.

It is believed that it is this interrelationship between the amount of beta phase present and hence the amount of Magnesium present in the alpha solid solution which leads to the observed deviation from a linear fit in figure 25. Second, there exists a possibility that the variable true stress plays more of a role than that suggested in equation (3). Therefore one might expect that equation (3) could be more correctly written in the following manner:

$$\dot{\epsilon} = K g(f_\beta, \sigma) (\sigma/\epsilon)^{1/m} \exp(-Q/RT) \quad (6)$$

wherein the function  $g(f_\beta, \sigma)$  is a parameter dependent upon the fraction of beta phase present (which in itself is a function of temperature) and also dependent on stress as



higher stress would in fact promote a finer particle size. Recalling the strain softening phenomenon observed in figures 20 and 21, which was manifest in a continuous decrease in stress with increasing strain at elevated temperatures, it becomes apparent that this material was undergoing microstructural changes while the test was in progress. So not only is there a continuous change in the fraction of beta phase present due to temperature, but there appears to be additional particle refinement while testing is in progress. It is this change in microstructure which leads to the anomalous behavior of the activation energies seen in figure 25.



#### D. FOLLOW ON ANALYSIS

In an attempt to better understand the microstructural dynamics during the compression testing phase, one of the test specimens, which was tested at 425° C and at the lowest strain rate used, was prepared and analyzed microscopically. Figures 27 through 30 are SEM photomicrographs taken at magnifications up to 12,500X of the above specimen. By comparing figures 27 and 28 to figures 15 and 16 (nearly the same magnifications), one may observe the striking changes evident in the microstructure of this post test specimen. Although the beta phase particles have enlarged (to an average size of about 1 micron), they are spread more uniformly throughout the alpha solid solution, providing a microstructure with enhanced homogeneity. Figures 29 and 30 show that the very fine, nonuniform particles observed in figures 17 and 18 have coalesced into somewhat larger, more uniform, spheroidized particles. Thus it is obvious that the structure has in fact changed during the course of the testing.

Based upon Bly, Sherby, and Young's (1) comments regarding a fine, spheroidized microstructure, it appears that this material approaches those ideal microstructural properties which provide for enhanced mechanical properties of increased strength and ductility. These properties are attainable through optimal thermal mechanical processes.



#### IV. CONCLUSIONS AND RECOMMENDATIONS

##### A. CONCLUDING COMMENTS

In concluding this research project there are two realizations of utmost significance which cannot be over emphasized. The first is that even though rudimentary in nature, the thermal mechanical process applied to this Aluminum-18 weight percent Magnesium alloy provided exciting results. Specifically, a 20% improvement in the strength to weight ratio over commercial high strength Aluminum alloys is achievable, not to mention enhanced ductility and toughness characteristics. The second realization is that the microstructure of this two phase proeutectic alloy can be controlled through thermal mechanical processing, leading one to expect that there does exist an optimum combination of thermal mechanical history and metallurgical composition which will result in the optimum high strength to weight Aluminum-Magnesium alloy.



## B. RECOMMENDATIONS

It appears that the surface has just been scratched and that there is much work to be done if that optimum microstructure is to be found. It is therefore heartily recommended that this effort not stop here but continue at an accelerated pace in an endeavor to find the optimum microstructure to provide that high strength to weight material so much a necessity in the Navy of today.



### Al-Mg      Aluminum-Magnesium

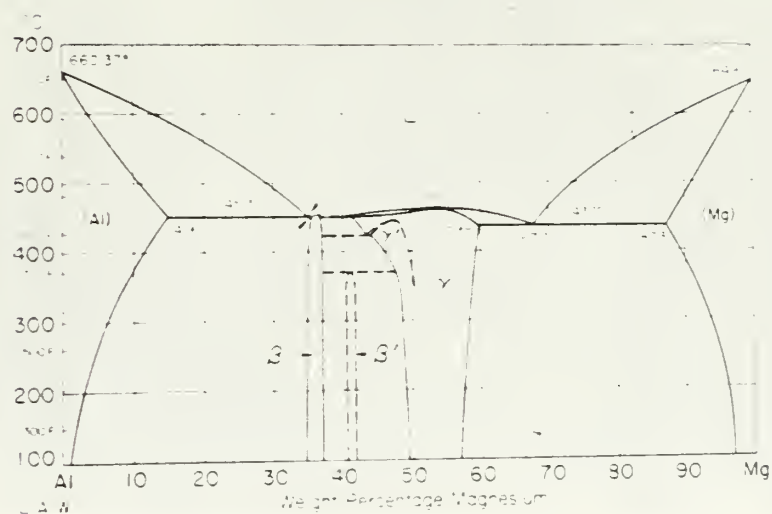


Figure 1 - ALUMINUM-MAGNESIUM PHASE DIAGRAM.





Figure 2 - MELTING FURNACE AND CLAY GRAPHITE CRUCIBLE.



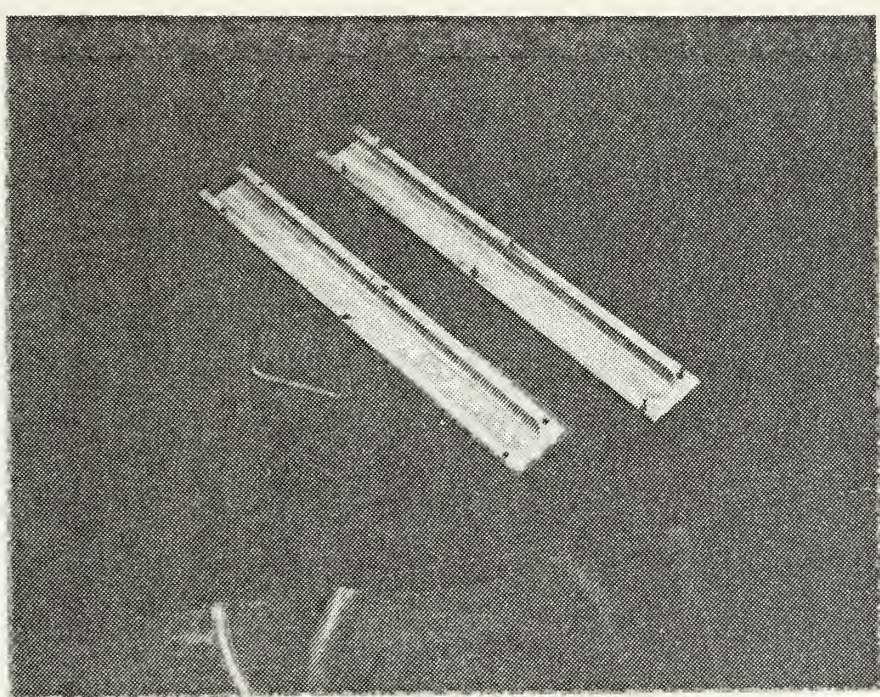


Figure 3 - SPLIT BRONZE MOLD, 1 INCH SQUARE BY 12 INCHES.



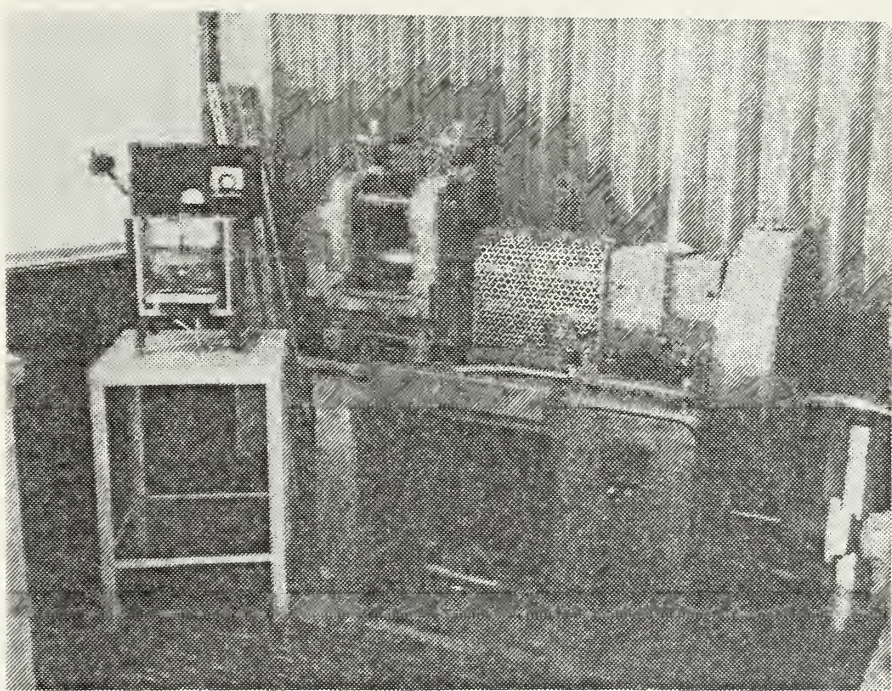


Figure 4 - WARMING FURNACE AND ROLLING MILL.



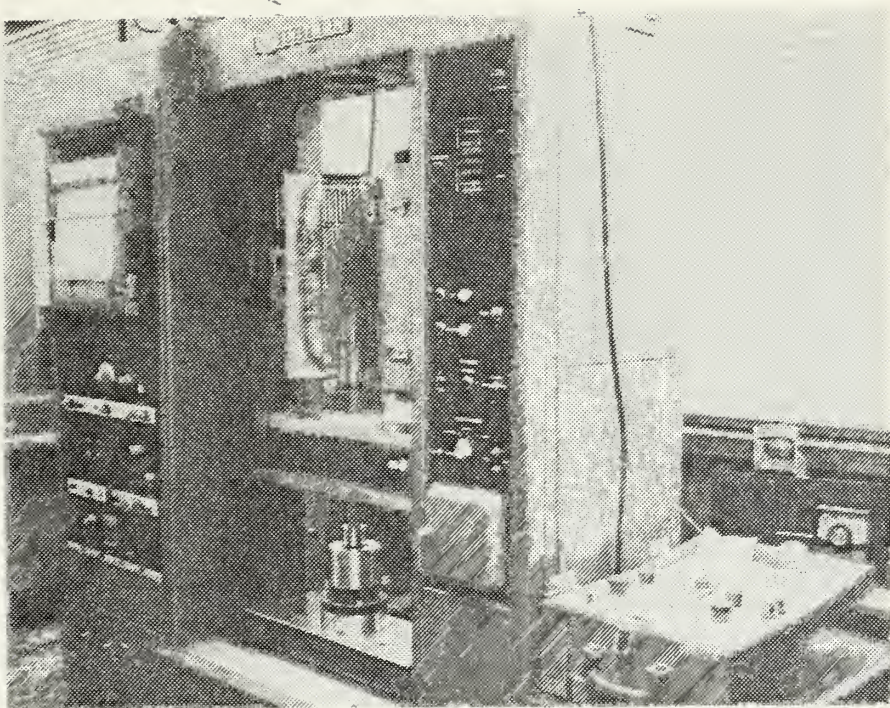


Figure 5 - INSTRON MODEL TT-D FLOOR MODEL TESTING MACHINE.



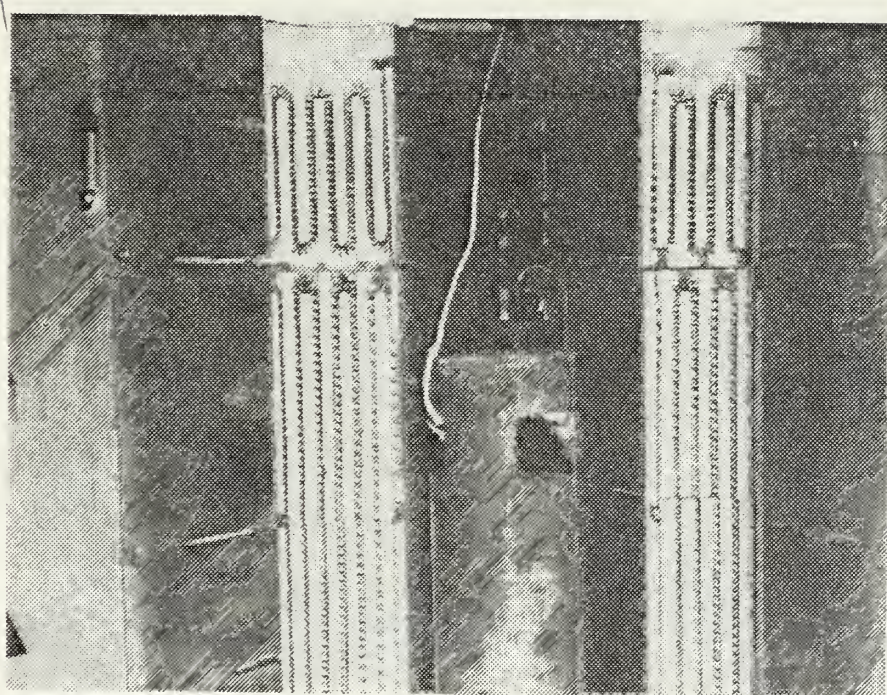


Figure 6 - SPECIAL COMPRESSION TEST ASSEMBLY WITH SUPPORT RING AND RETAINING CLIPS.



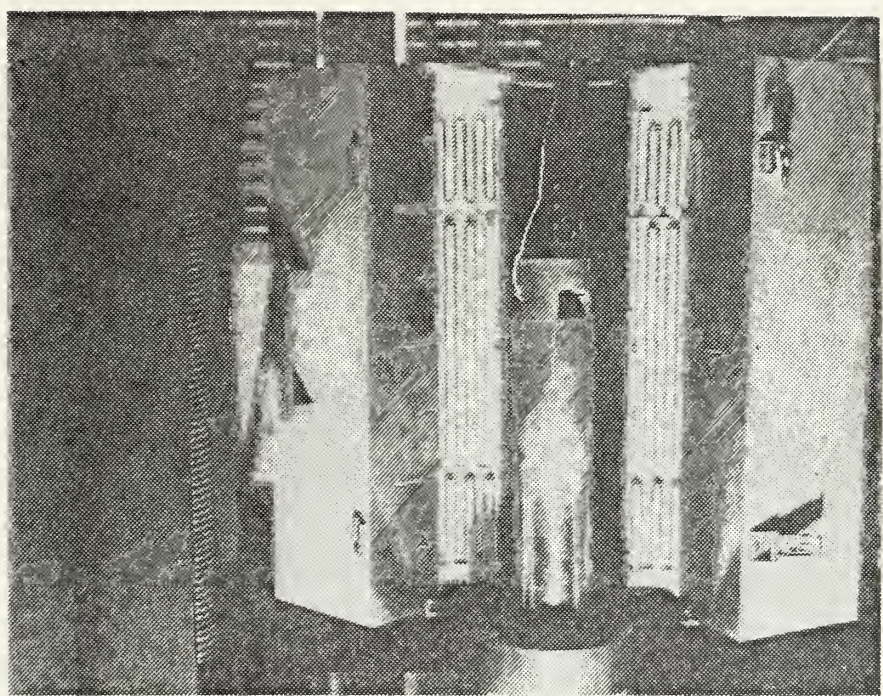


Figure 7 - MARSHALL SPLIT FURNACE.



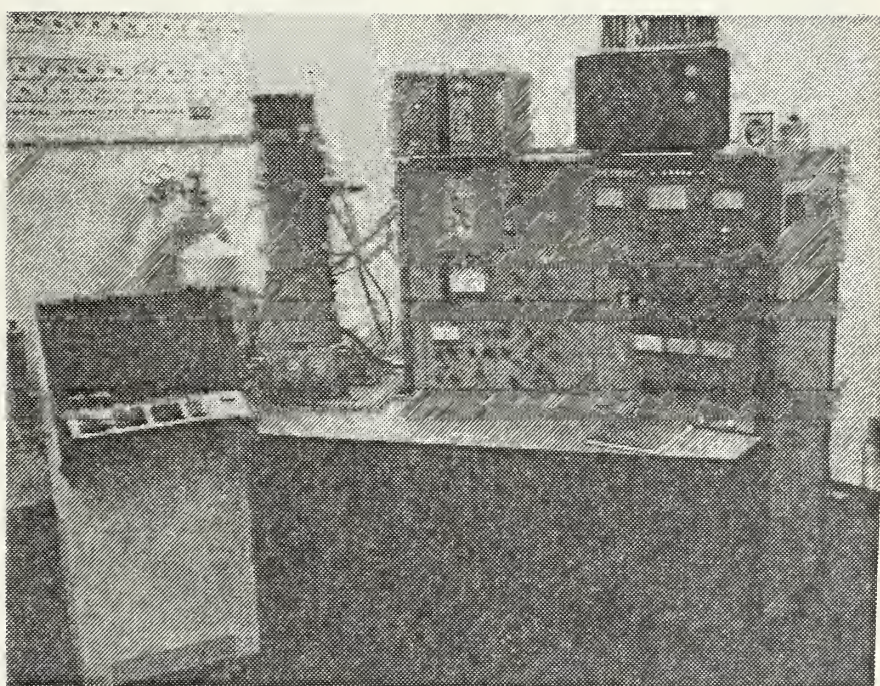


Figure 8 - S4-10 STEREOSCAN SCANNING ELECTRON MICROSCOPE  
WITH PGT-1000 MICRO ANALYSIS SYSTEM.



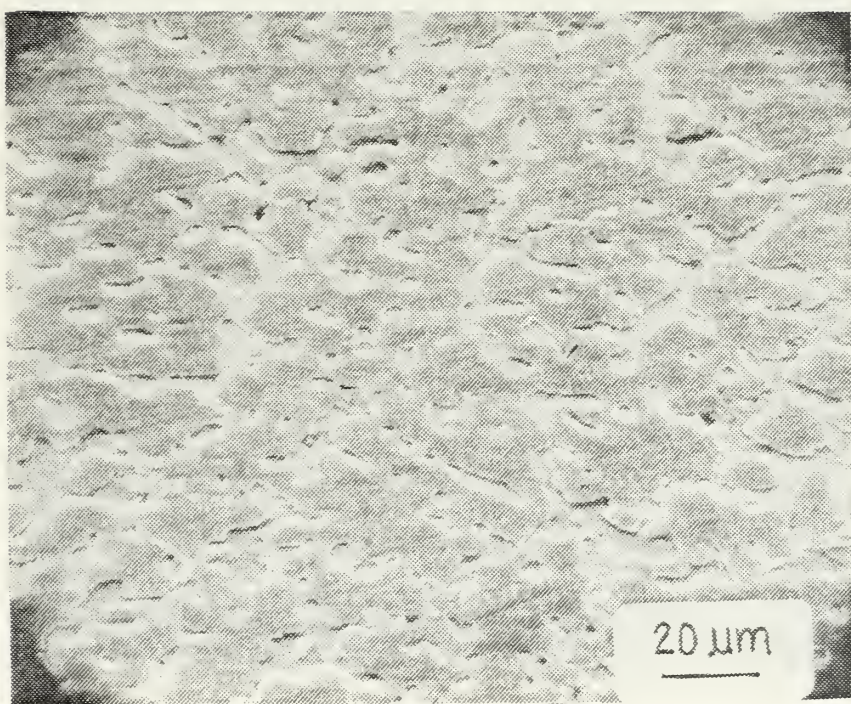


Figure 9 - SEM PHOTOGRAPH OF AS CAST MATERIAL, 610X.



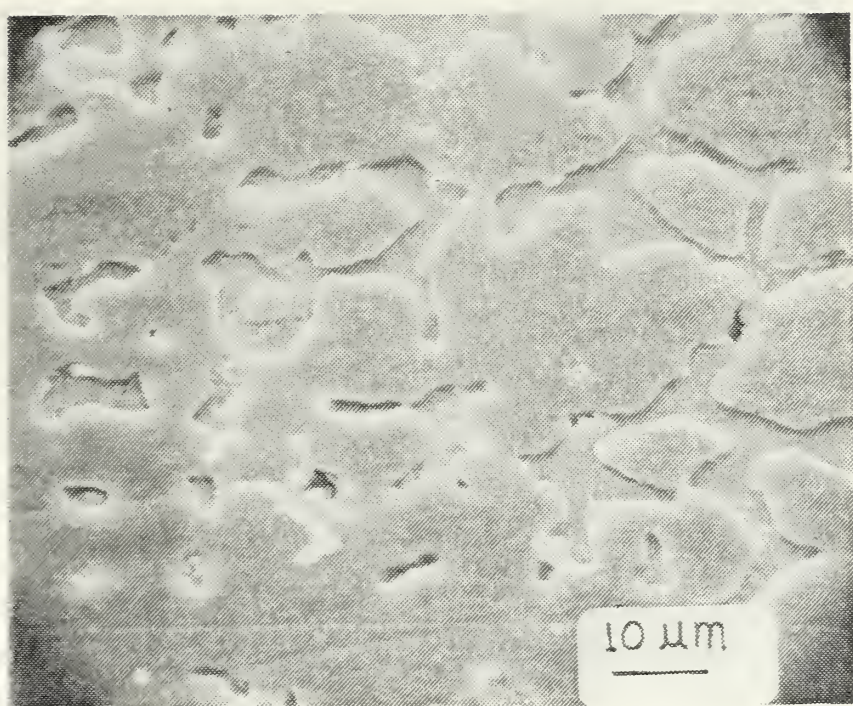


Figure 10 - SEM PHOTOGRAPH #1 OF AS CAST MATERIAL, 1,200X.



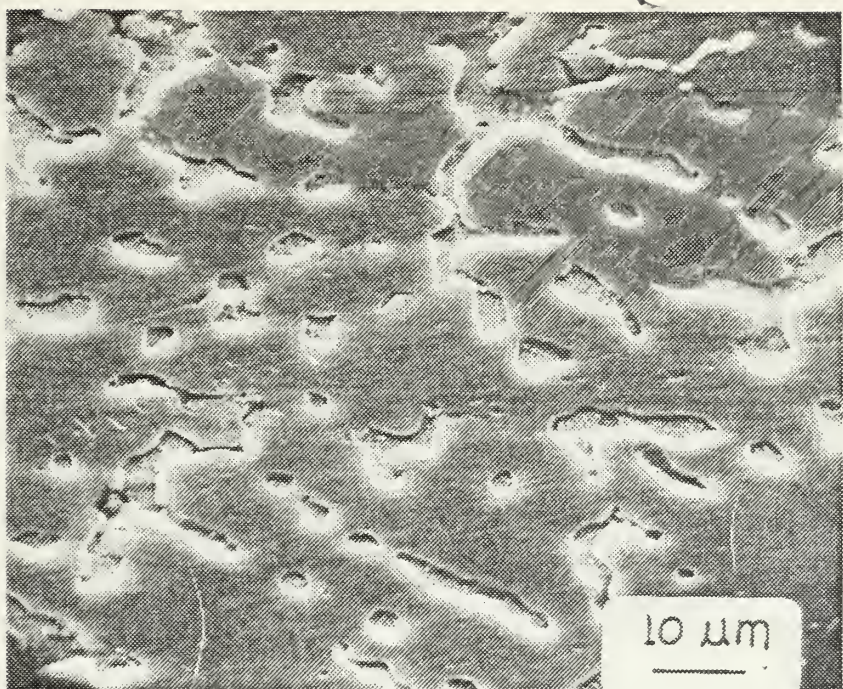


Figure 11 - SEM PHOTOGRAPH #2 OF AS CAST MATERIAL, 1,200X.



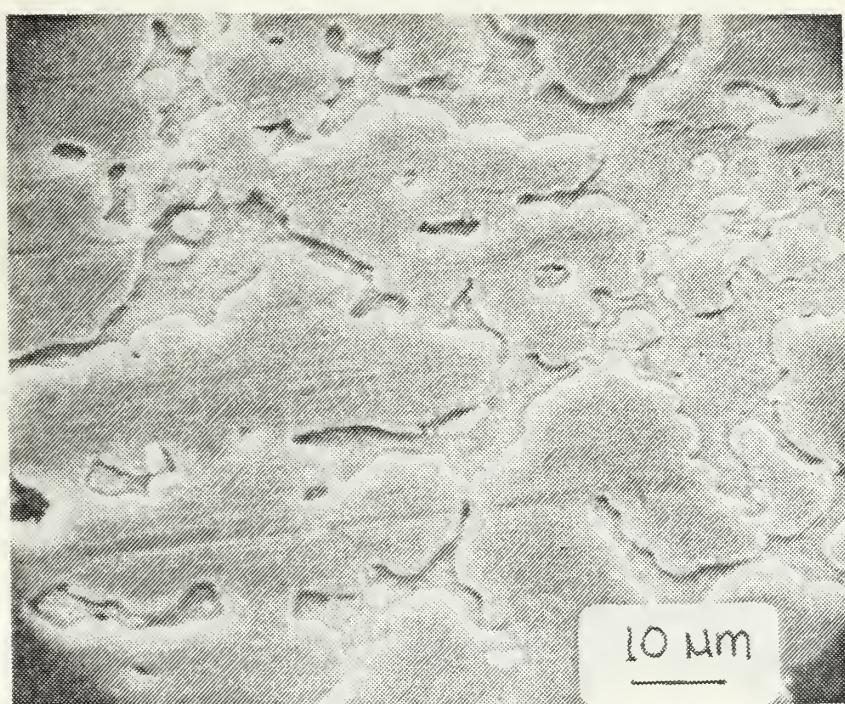


Figure 12 - SEM PHOTOGRAPH #3 OF AS CAST MATERIAL, 1,200X.



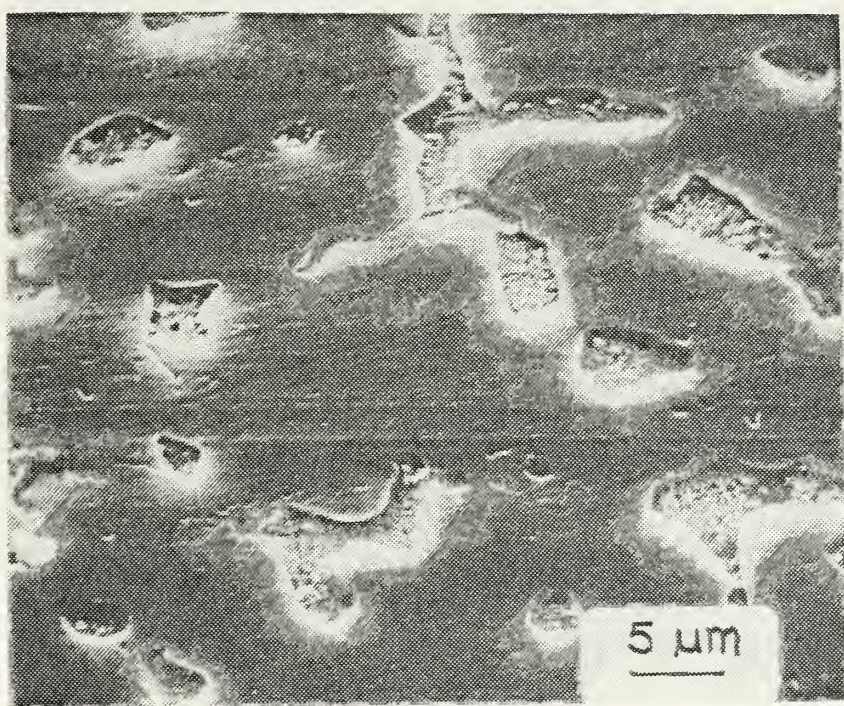


Figure 13 - SEM PHOTOGRAPH #1 OF AS CAST MATERIAL, 2,400X.



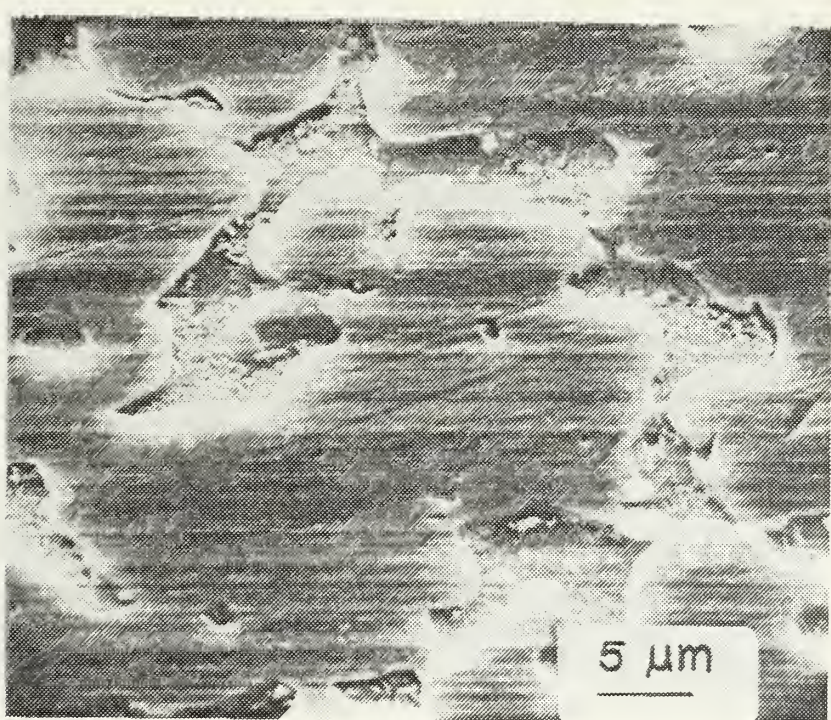


Figure 14 - SEM PHOTOGRAPH #2 OF AS CAST MATERIAL, 2,400X.



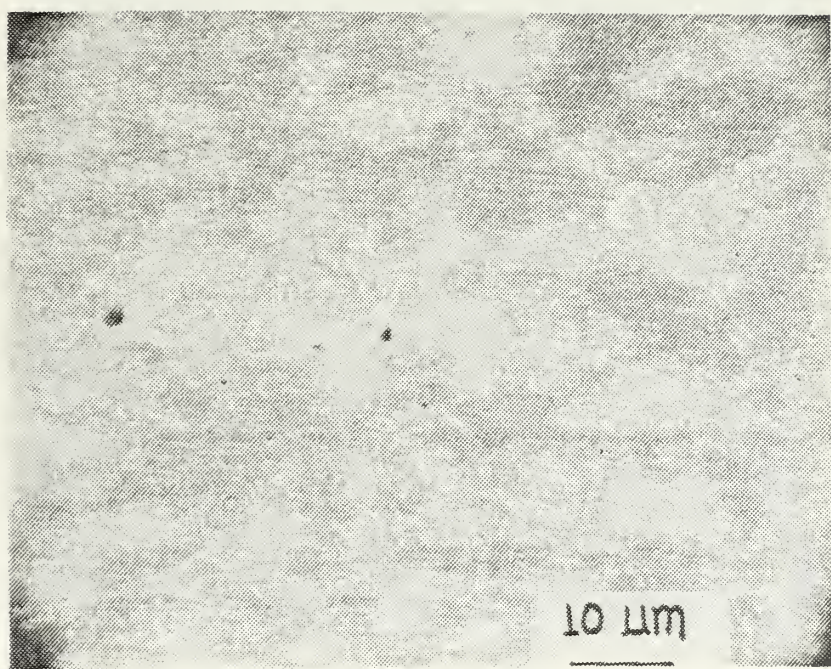


Figure 15 - SEM PHOTOGRAPH OF WARM ROLLED MATERIAL, 1,280.



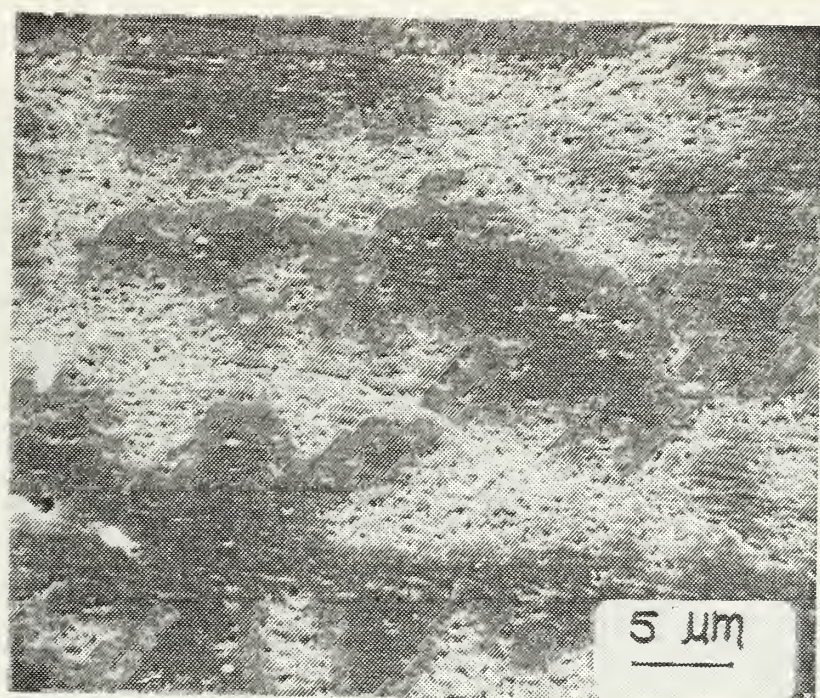


Figure 16 - SEM PHOTOGRAPH OF WARM ROLLED MATERIAL, 2,550X.



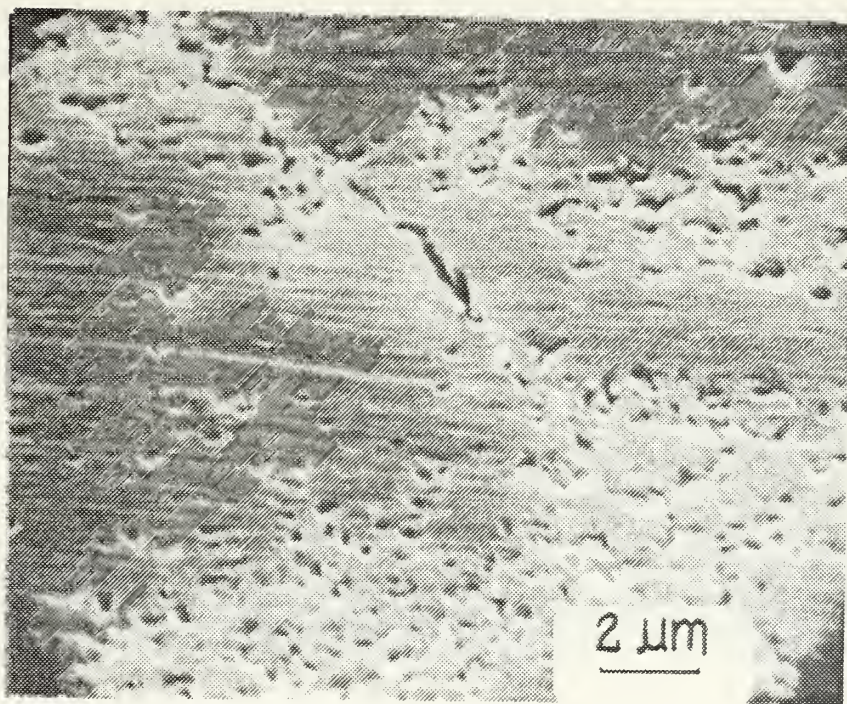


Figure 17 - SEM PHOTOGRAPH OF WARM ROLLED MATERIAL, 6,300X.



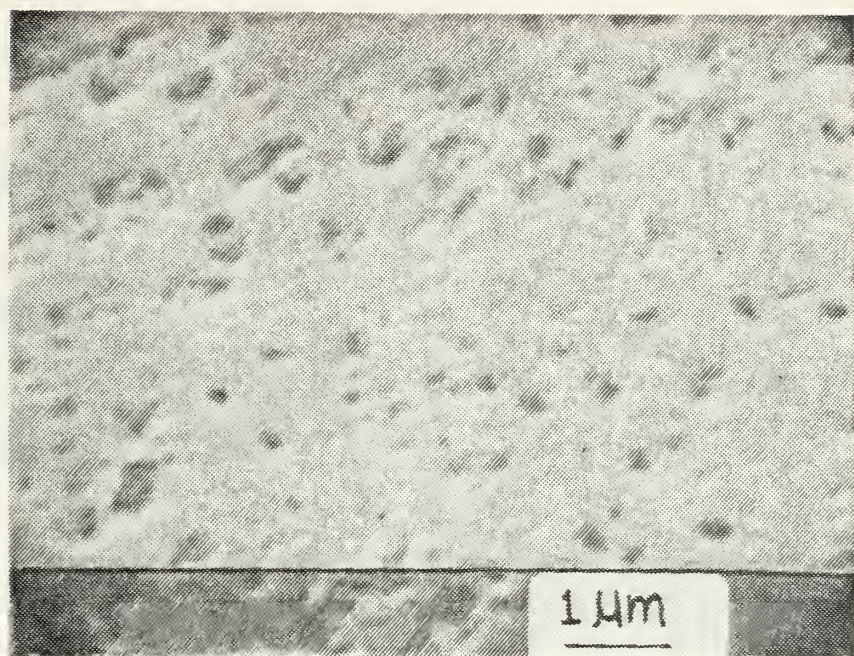


Figure 18 - SEM PHOTOGRAPH OF WARM ROLLED MATERIAL,  
13,000X.



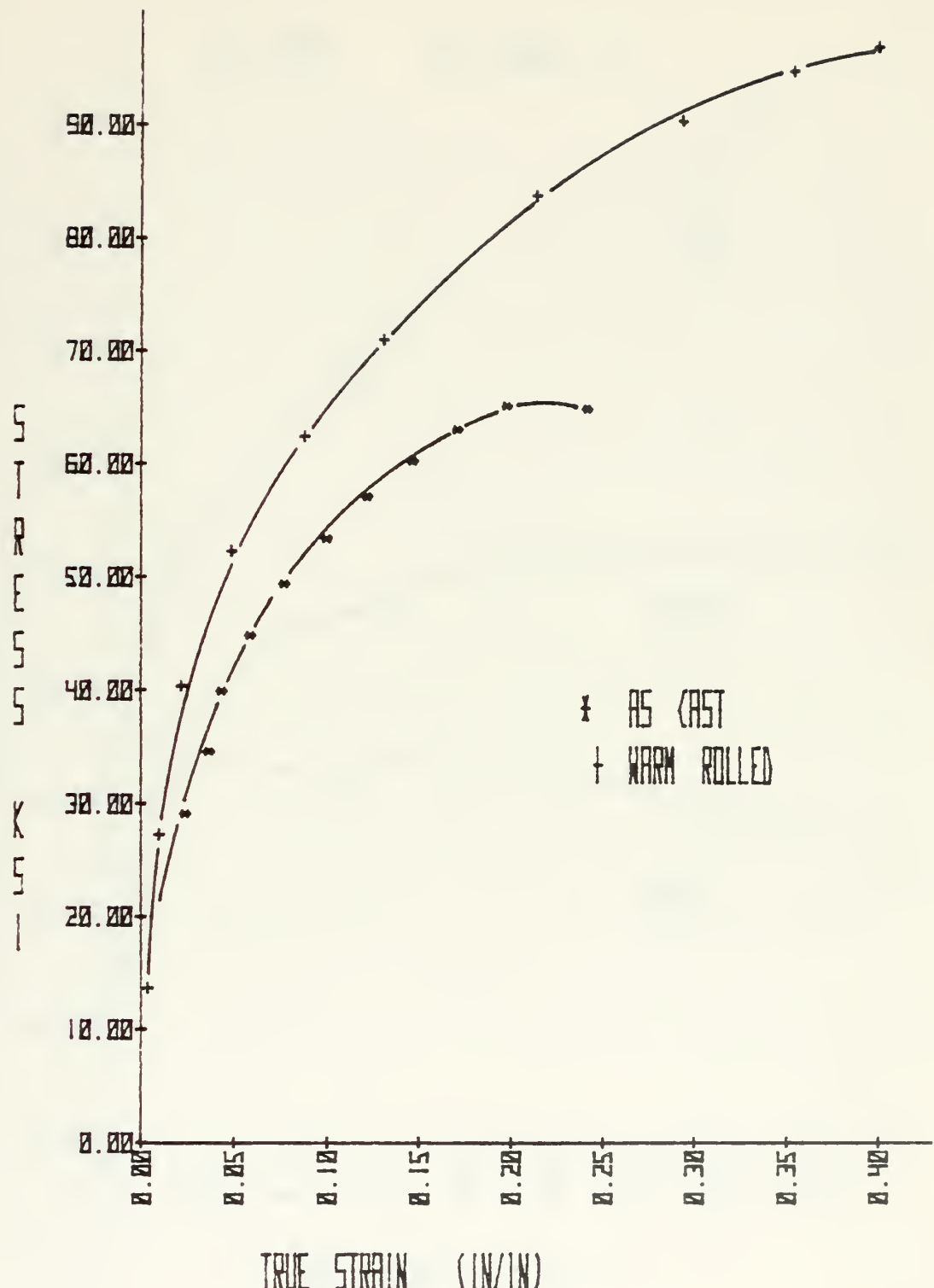


Figure 19 - TRUE STRESS VS. TRUE STRAIN FOR AS CAST (\*) AND WARM ROLLED (+) MATERIAL.



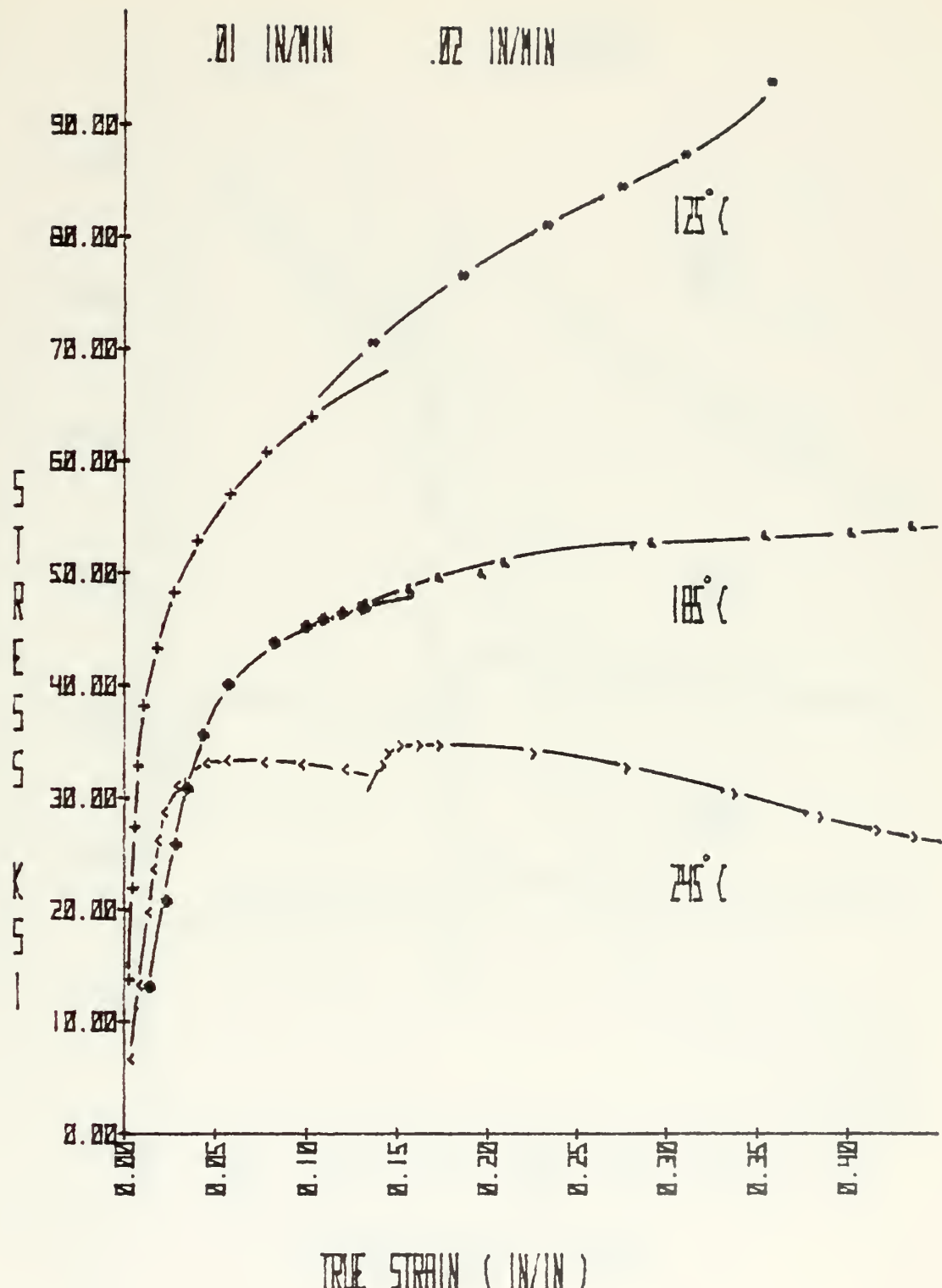


Figure 20 - TRUE STRESS VS. TRUE STRAIN FOR WARM ROLLED MATERIAL AT TWO CROSS HEAD SPEEDS AND TEMPERATURES TO 245°C.



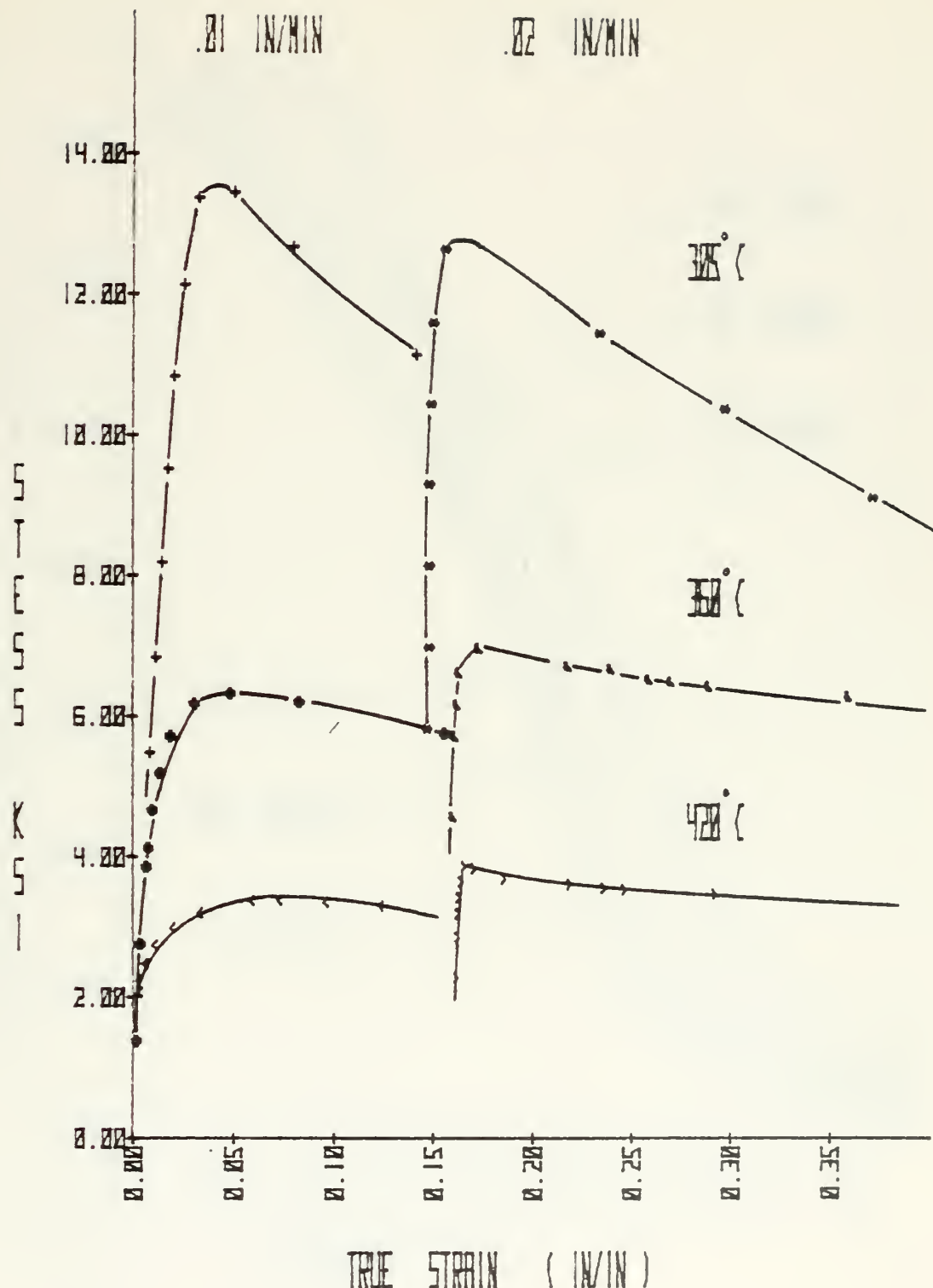


Figure 21 - TRUE STRESS VS. TRUE STRAIN FOR WARM ROLLED MATERIAL AT TWO CROSS HEAD SPEEDS AND TEMPERATURES TO 420° C.



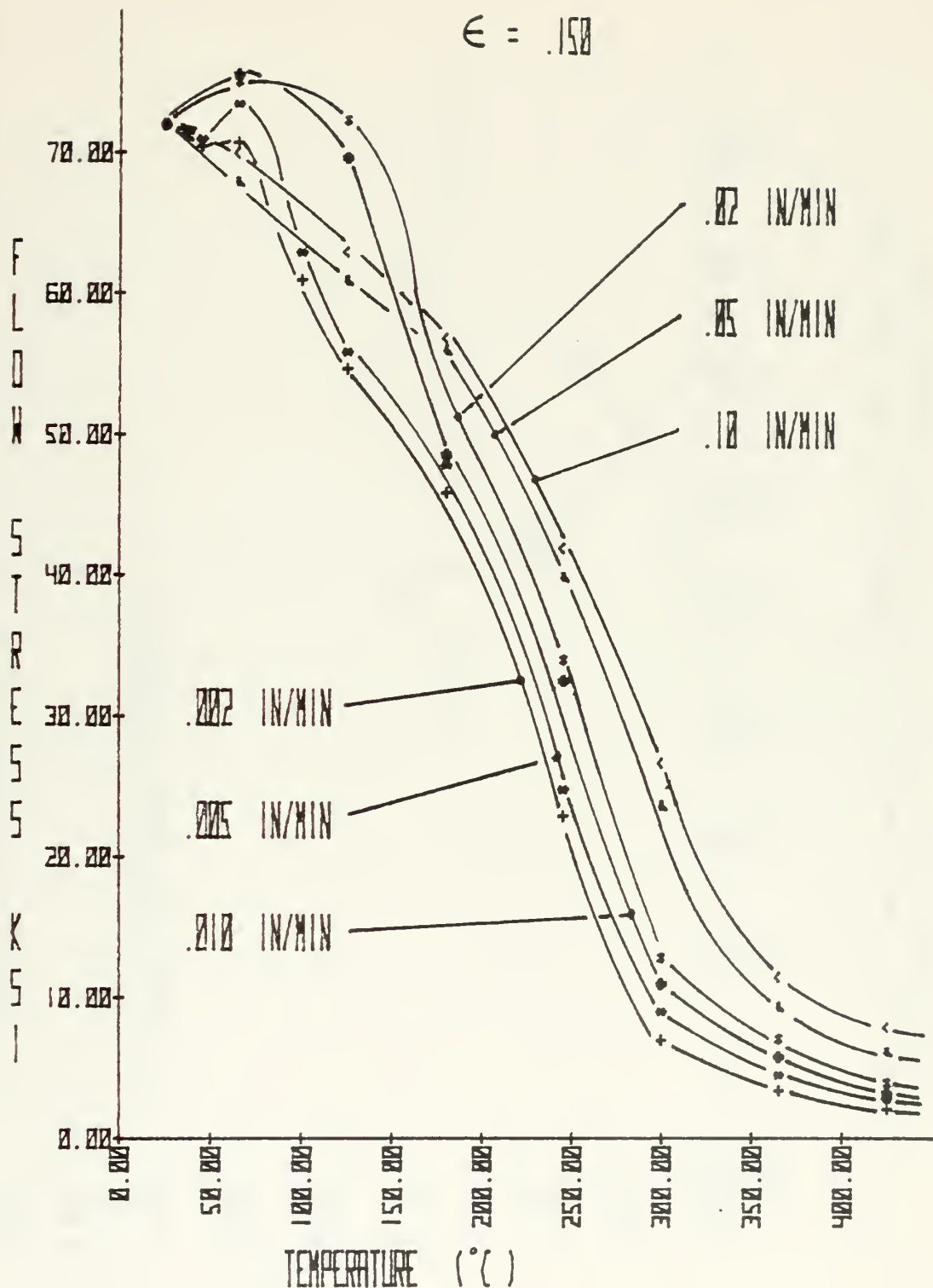


Figure 22 - FLOW STRESS VS. TEMPERATURE AT A TRUE STRAIN OF 0.15 FOR SIX STRAIN RATES.



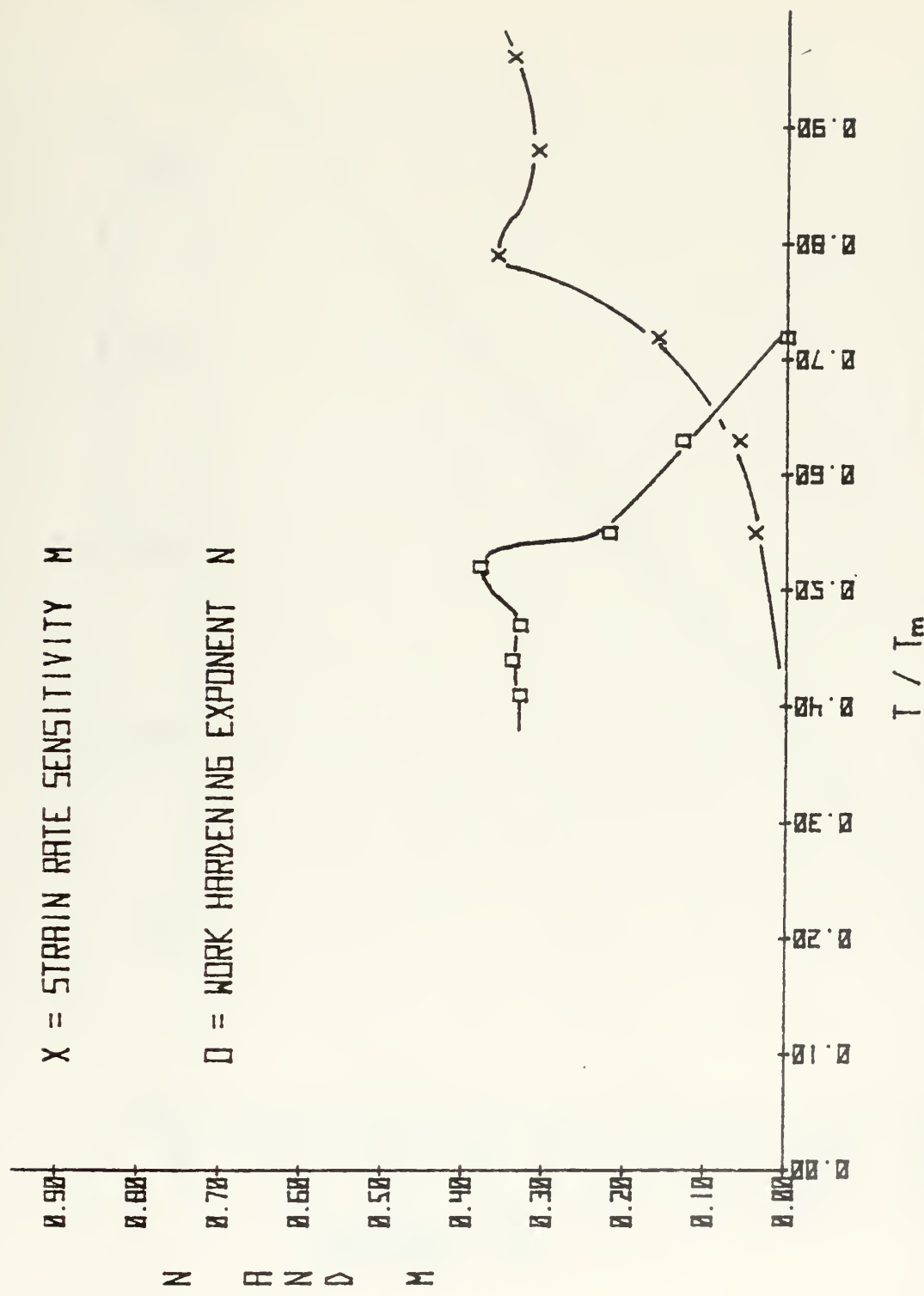


Figure 23 - WORK HARDENING EXPONENT (n) AND STRAIN RATE SENSITIVITY (m) VS. FRACTION OF ABS. MELTING TEMP.



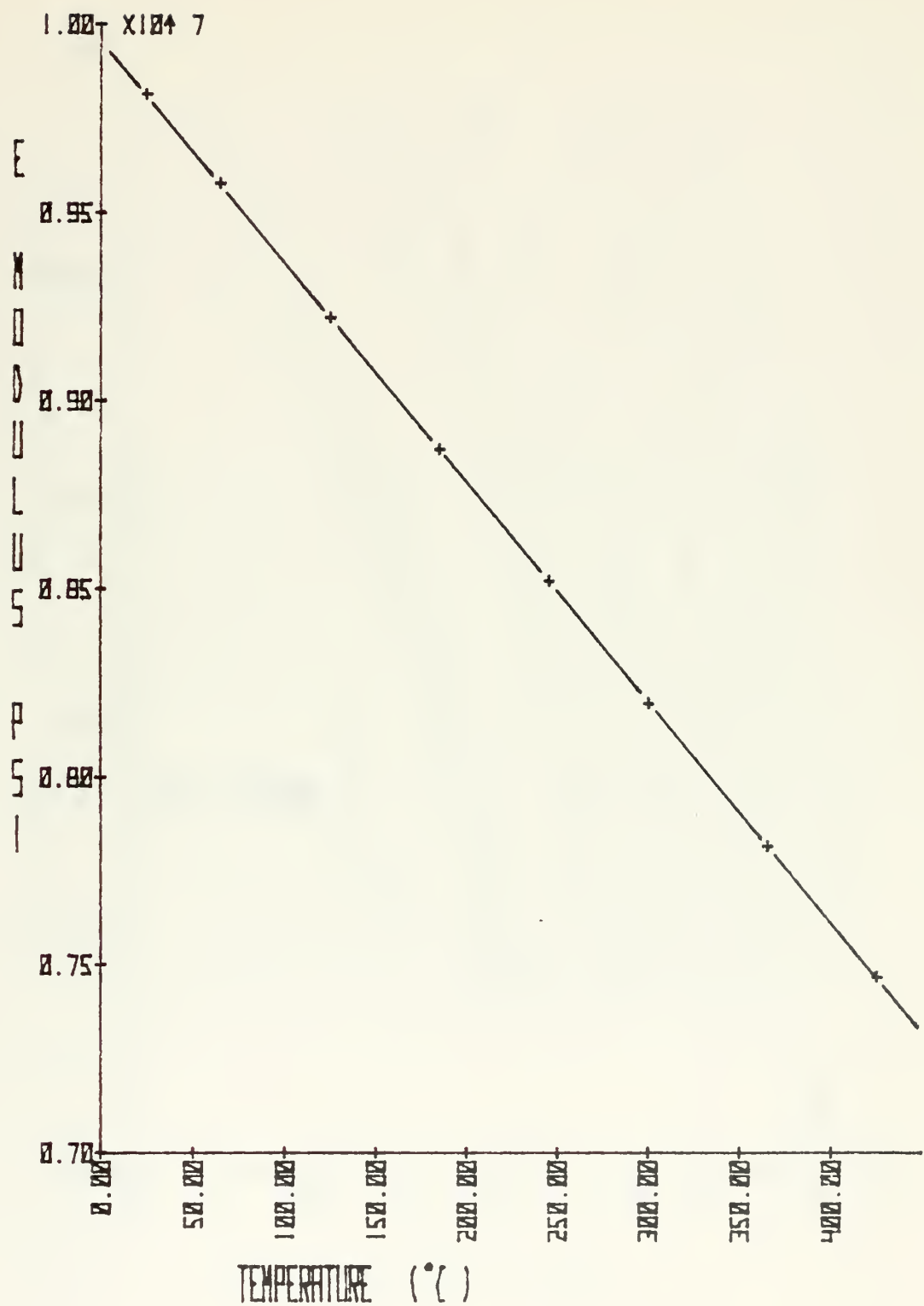


Figure 24 - ELASTIC MODULUS (E) VS. TEMPERATURE, (11).



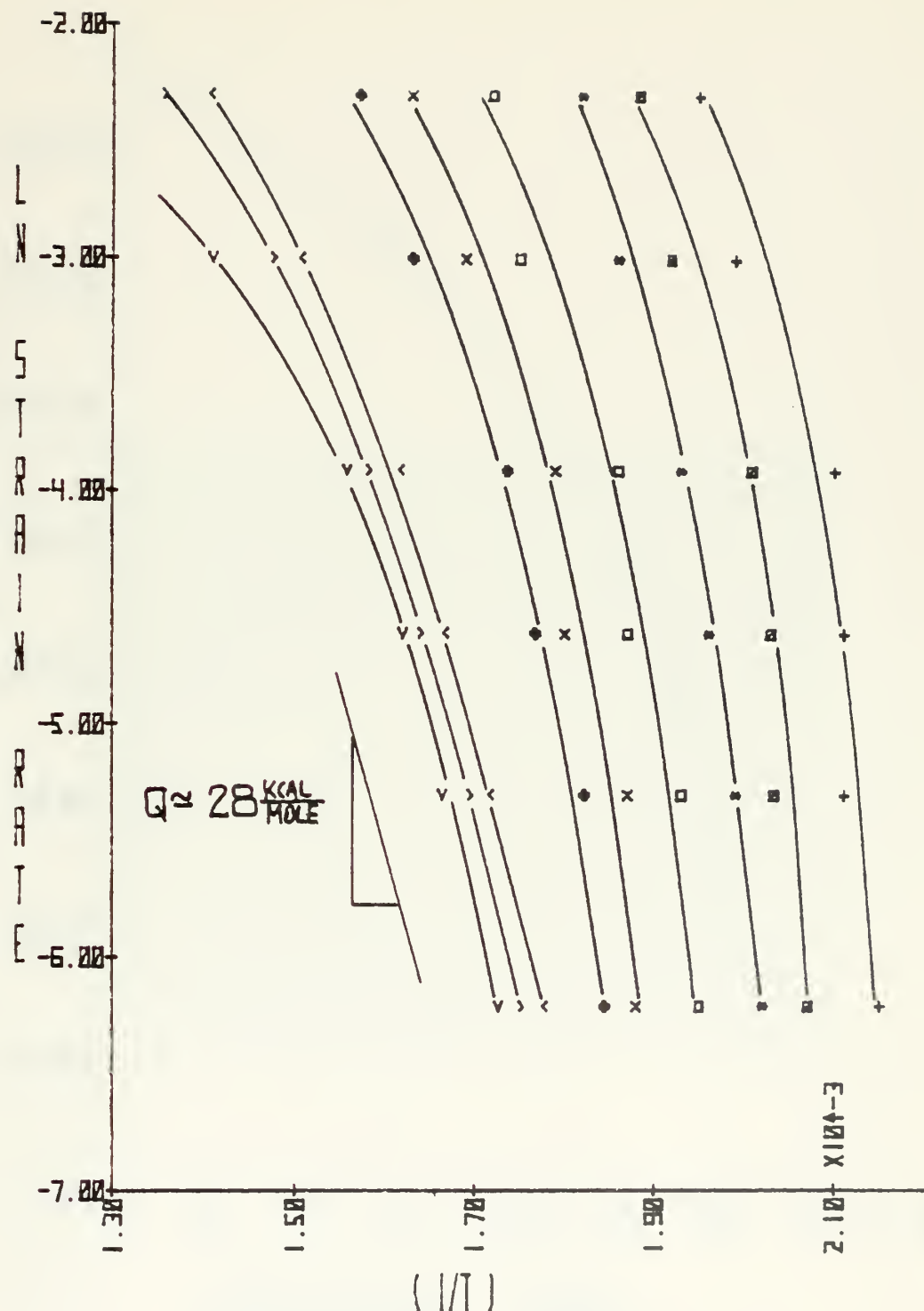


Figure 25 - NATURAL LOG OF STRAIN RATE VS. RECIPROCAL ABSOLUTE TEMPERATURE FOR VARIOUS VALUES OF  $(\sigma/E)$ .



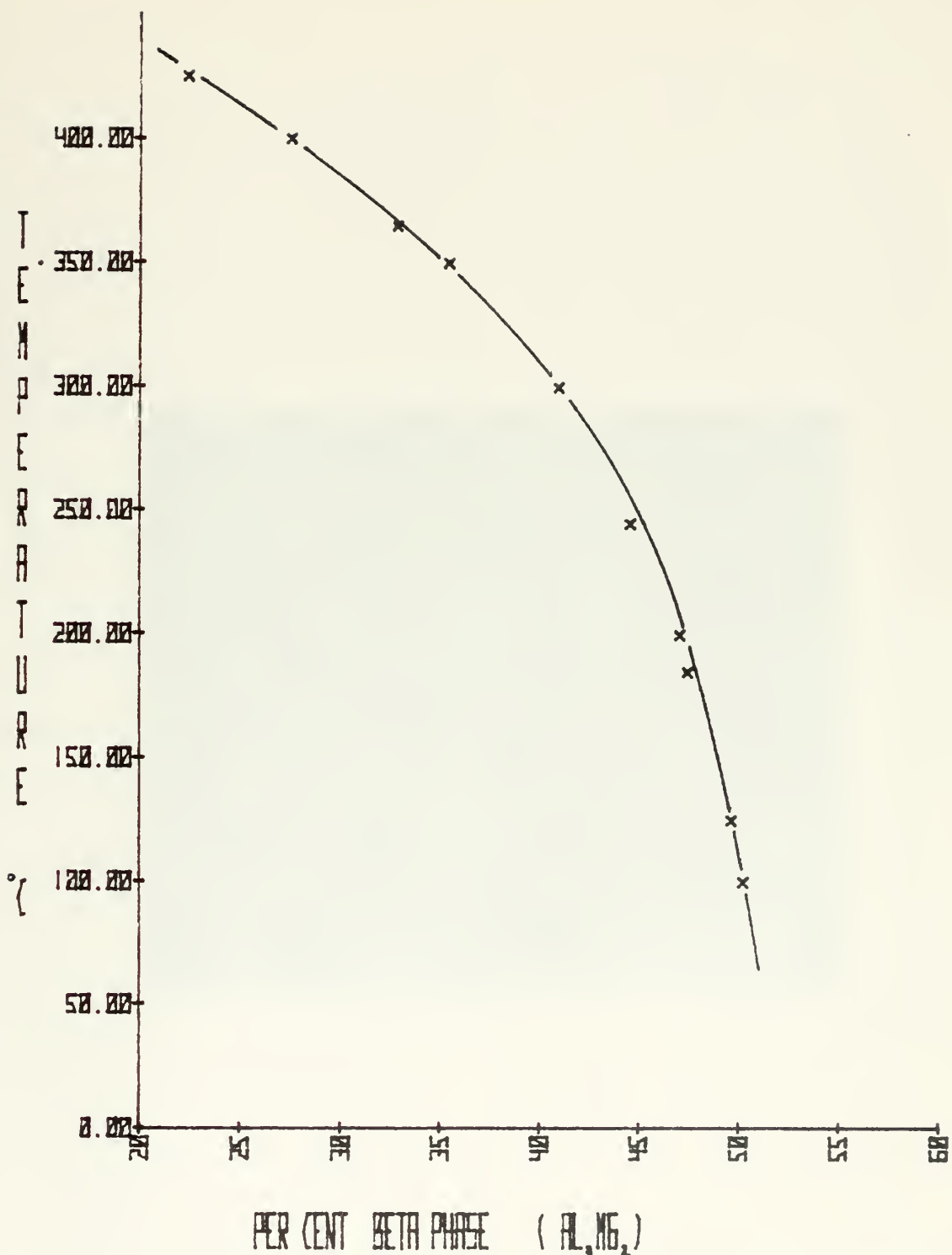


Figure 26 - TEMPERATURE VS. PERCENTAGE BETA PHASE  
INTERMETALLIC.



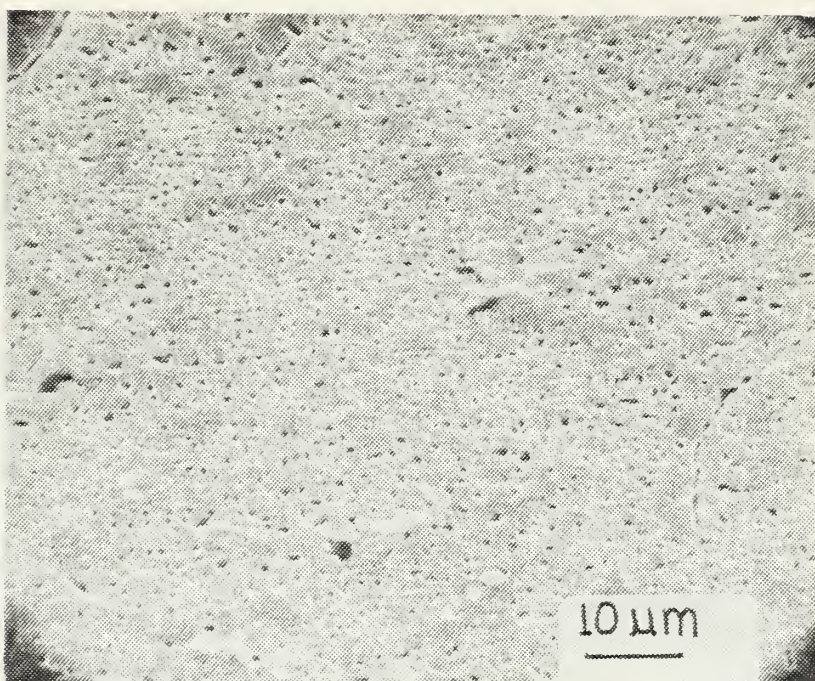


Figure 27 - SEM PHOTOGRAPH OF A WARM ROLLED SPECIMEN FOLLOWING COMPRESSION TESTING, 1,225X.



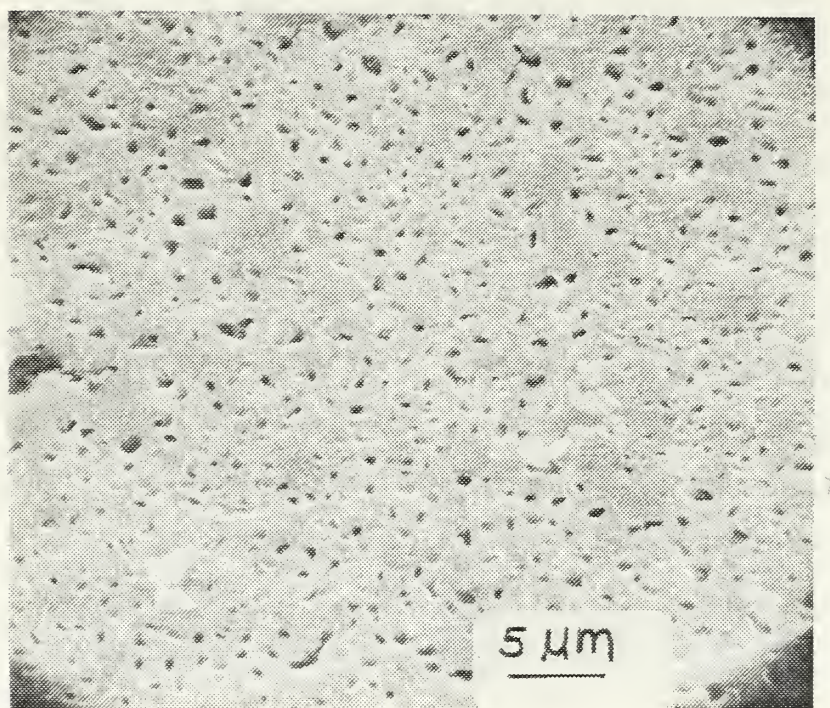


Figure 28 - SEM PHOTOGRAPH OF A WARM ROLLED SPECIMEN  
FOLLOWING COMPRESSION TESTING, 2,500X.



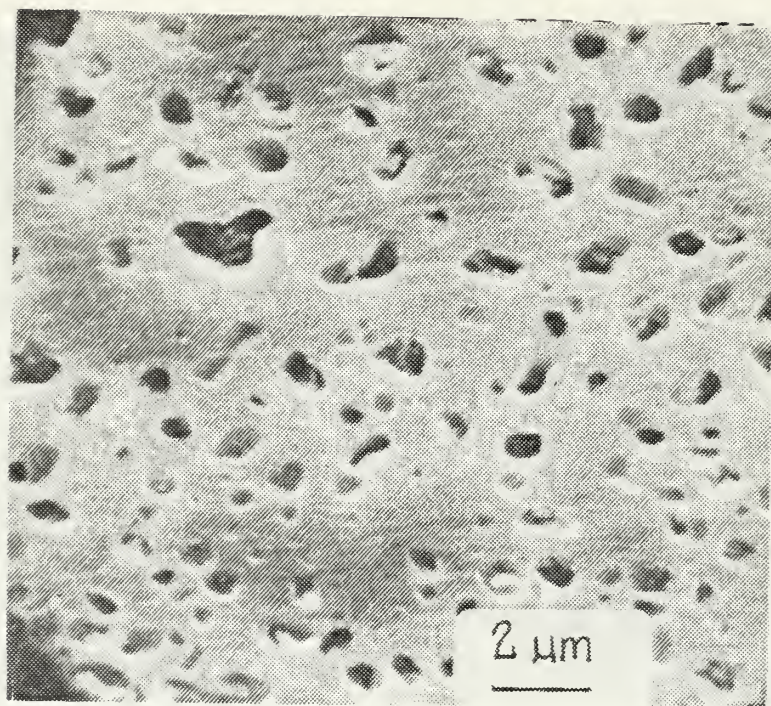


Figure 29 - SEM PHOTOGRAPH OF A WARM ROLLED SPECIMEN  
FOLLOWING COMPRESSION TESTING, 6,300X.



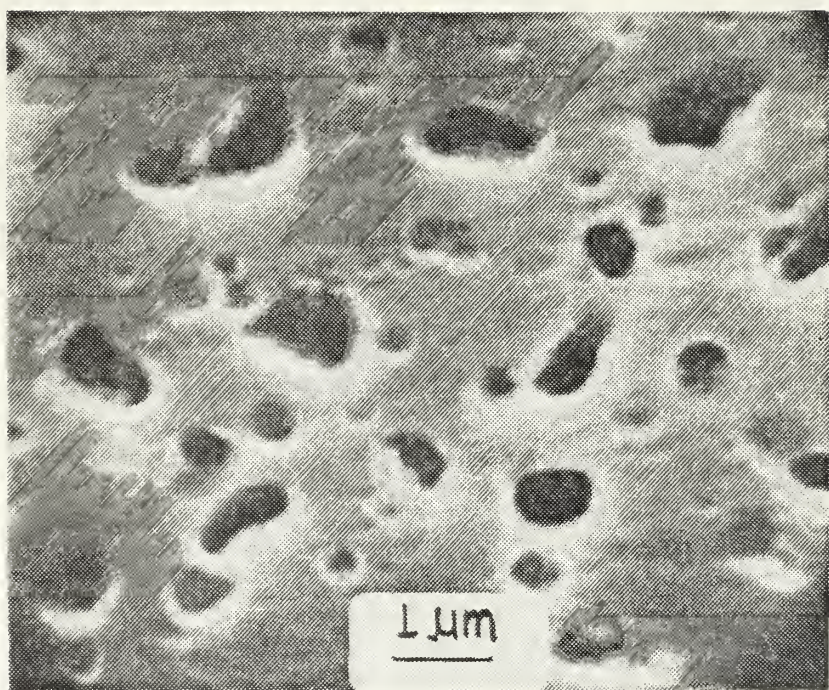


Figure 30 - SEM PHOTOGRAPH OF A WARM ROLLED SPECIMEN FOLLOWING COMPRESSION TESTING, 12,500X.



## APPENDIX A

### ALUMINUM-MAGNESIUM CASTING PROCEDURES

1. Outgas carbon crucible for one hour at 250° C.
2. Charge crucible with Aluminum, and place it in furnace preheated to 750° C and continuously flushed with dry Argon.
3. In about one hour remove crucible, stir and flux with about 0.2 ounce of "Coverall #33FF."
4. Submerge the Magnesium pieces into the molten Aluminum with stainless steel tongs. Return crucible to furnace.
5. In about thirty minutes remove crucible, again flux with 0.2 ounce of "Coverall #33FF" and carefully stir.
6. Remove dross from surface with stainless steel scoop; return crucible to furnace.
7. In approximately twenty minutes remove crucible, and pour melt into mold.



## LIST OF REFERENCES

1. D. L. Bly, O. D. Sherby and C. M. Young, "Influence of Thermal Mechanical Treatments on the Mechanical Properties of a Finely Spheroidized Eutectic-Composition Steel", Materials Science and Engineering, v. 12, p. 41-46, 1973.
2. O. D. Sherby, "Superplasticity of Metals and Alloys", ARPA Workshop Presentation, v. 1, p. 1-17, 1976.
3. Taylor Lyman, Metals Handbook Volume 5, p. 433-435, American Society for Metals, 1970.
4. G. L. Kehl, Metallographic Laboratory Practice, p. 71,72,424, McGraw-Hill, 1949.
5. A. G. Guy and J. J. Hren, Elements of Physical Metallurgy, p. 228-235, Addison-Wesley, 1974.
6. Taylor Lyman, Metals Handbook Volume 8, p. 120-129,261, American Society for Metals, 1970.
7. G. E. Dieter, Mechanical Metallurgy, p. 340-344, McGraw-Hill, Inc., 1961.
8. O. Sherby and P. Burke, "Mechanical Behavior of Crystalline Solids at Elevated Temperature", Progress in Materials Science, v. 13, p. 325-390, 1968.
9. C. L. Meyers, J. C. Shyne and O. D. Sherby, "Temperature Dependence of Steady State Creep on Aluminum Alloys", J. Aust. Inst. Metals, v. 12, p. 171, 1963.
10. C. R. Barrett, W. D. Nix, and A. S. Tetelman, The



Principles of Engineering Materials, p. 230-268,  
Prentice-Hall, Inc., 1973.

11. M. Fine, "Apparatus for Precise Determination of Dynamic Youngs Modulus and Internal Friction at Elevated Temperatures", The Review of Scientific Instruments, v. 28, p. 643, 1957.



INITIAL DISTRIBUTION LIST

	No. Copies
1. Defense Documentation Center .	2
Cameron Station	
Alexandria, Virginia 22314	
2. Library, Code 0212	2
Naval Postgraduate School	
Monterey, California 93940	
3. Department Chairman, Code 69	2
Department of Mechanical Engineering	
Naval Postgraduate School	
Monterey, California 93940	
4. Professor T. R. McNelley, Code 69Mc	2
Department of Mechanical Engineering	
Naval Postgraduate School	
Monterey, California 93940	
5. Professor A. J. Perkins, Code 69Ps	2
Department of Mechanical Engineering	
Naval Postgraduate School	
Monterey, California 93940	
6. Professor G. R. Edwards	2
Department of Metallurgical Engineering	
Colorado School of Mines	
Golden, Colorado 80401	
7. Lt. Frank G. Ness Jr.	2
5140 Los Robles Drive	
Carlsbad, California 92008	











4 APR 78

S11822

Thesis

N413

c.1 Ness

16890

High strength to  
weight aluminum-18  
weight percent magnesium  
alloy through thermal  
mechanical processing.

4 APR 78

S11822

Thesis

168861

N413

Ness

c.1

High strength to  
weight aluminum-18  
weight percent magnesium  
alloy through thermal  
mechanical processing.

thesN413  
High strength to weight aluminum-18 weig



3 2768 001 89907 3  
DUDLEY KNOX LIBRARY C.9